Adaptive-optics ultrahigh-resolution optical coherence tomography

B. Hermann
Department of Medical Physics, Christian Doppler Laboratory, Medical University of Vienna, Austria

E. J. Fernández
Laboratorio de Óptica, Departamento de Física, Universidad de Murcia, Campus de Espinardo, Murcia, Spain

A. Unterhuber, H. Sattmann, A. F. Fercher, and W. Drexler
Department of Medical Physics, Christian Doppler Laboratory, Medical University of Vienna, Austria

P. M. Prieto and P. Artal
Laboratorio de Óptica, Departamento de Física, Universidad de Murcia, Campus de Espinardo, Murcia, Spain

Received March 22, 2004

Merging of ultrahigh-resolution optical coherence tomography (UHR OCT) and adaptive optics (AO), resulting in high axial (3 μm) and improved transverse resolution (5–10 μm) is demonstrated for the first time to our knowledge in *in vivo* retinal imaging. A compact (300 mm × 300 mm) closed-loop AO system, based on a real-time Hartmann–Shack wave-front sensor operating at 30 Hz and a 37-actuator membrane deformable mirror, is interfaced to an UHR OCT system, based on a commercial OCT instrument, employing a compact Ti:sapphire laser with 130-nm bandwidth. Closed-loop correction of both ocular and system aberrations results in a residual uncorrected wave-front rms of 0.1 μm for a 3.68-mm pupil diameter. When this level of correction is achieved, OCT images are obtained under a static mirror configuration. By use of AO, an improvement of the transverse resolution of two to three times, compared with UHR OCT systems used so far, is obtained. A significant signal-to-noise ratio improvement of up to 9 dB in corrected compared with uncorrected OCT tomograms is also achieved.

OCIS codes: 110.4500, 010.1080, 220.1000, 320.7090.

Optical coherence tomography[1] (OCT) is a well-established, promising diagnostic technique with many potential applications in biomedicine. A significant advance in *in vivo* visualization of intraretinal layers was recently achieved by use of state-of-the-art ultrabroad-bandwidth light sources, demonstrating the potential of ultrahigh-resolution OCT[2] (UHR OCT) to perform noninvasive optical biopsy of the human retina.[3]

The transverse resolution in ophthalmic UHR OCT is determined by the smallest achievable spot size on the retina. In a diffraction-limited eye, a 4-mm-diameter beam (with a center wavelength of 800 nm) would produce a theoretical spot size of 4.3 μm. However, in practice, for large pupil diameters, monochromatic aberrations of the eye[4] blur the retinal images. Although the axial resolution of ophthalmic OCT has been improved dramatically, the transverse resolution is still limited to ~15–20 μm in retinal UHR OCT tomograms because of the small beam diameter (1 mm) used so far.

One promising approach to correcting ocular aberrations, to decrease the spot size at the retina and to therefore improve transverse resolution in UHR OCT, is the use of adaptive optics (AO).[5–9] Recently, there have also been first attempts at combining an *en face* coherence-gated camera with AO for *en face* OCT imaging[10] with standard axial resolution (14 μm) and high transverse resolution. In this Letter we demonstrate, for the first time as far as we know, the combination of UHR OCT and AO for high axial and transverse-resolution *in vivo* retinal imaging.

A compact (300 mm × 300 mm) closed-loop AO system,[11] shown in Fig. 1, based on a real-time Hartmann–Shack (HS) wave-front sensor operating at 30 Hz and a 37-element low-cost micromachined membrane deformable mirror (OKO Technologies, Holland), was interfaced to a fiber-optic, time-domain UHR OCT system. The OCT system itself was based on a commercially available OCT 1 instrument (Carl Zeiss Meditec AG, Dublin, Calif.), employing a compact Ti:sapphire laser (FEMTOLASERS Produktions GmbH, Vienna, Austria) with 130-nm optical bandwidth (at FWHM) centered at 800 nm.

The AO system was designed to conjugate the exit pupil of the eye onto the deformable mirror, into the HS sensor, and into the fiber. The diameter of the measurement beam entering the eye was increased from 1 to 3.68. To keep the imaging planes during the

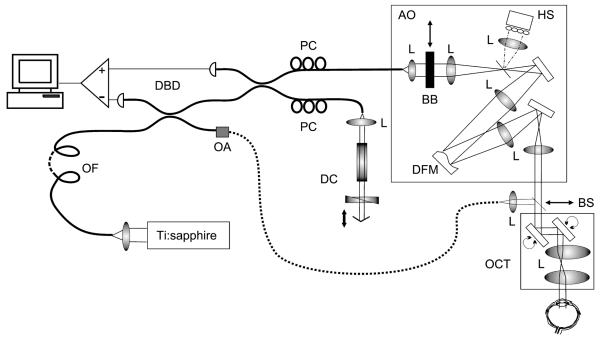

Fig. 1. AO UHR OCT system: DBD, dual balanced detection; PCs, polarization controllers; OA, optical attenuator; OF, 100 m of optical fiber; DC, dispersion compensation; L's, achromatic doublet lenses; BB, removable beam blocker; DFM, deformable mirror; BS, removable beam splitter.

0146-9592/04/182142-03$15.00/0

measurement and correction of ocular aberrations, the distance of the investigated eye to the exit lens of the OCT was set properly and kept constant. Accommodation was paralyzed with tropicamide (mydriacyl, Mydriaticum Agepha). Since the OCT system uses an off-center illumination geometry, there were no backreflections from the lenses of the OCT system. To prevent backreflections from lenses of the AO into the HS sensor, a probe beam that delivered 5 μW onto the eye was introduced at the entrance of the OCT system with a removable beam splitter while the OCT beam was blocked with a removable beam blocker. In this mode both the aberrations of the eye and those of the imaging optics were measured and corrected. Preliminary tests showed the procedure could be performed with the scanning probe beam in real time. When the correction was achieved, the system was switched to the UHR OCT imaging mode by removal of the beam blocker and the beam splitter. UHR OCT tomograms were acquired with corrected as well as uncorrected wave fronts with axial scan rates ranging from 125 to 250 Hz with up to 800 μW of incident optical power in the scanning OCT beam, well below the American National Standards Institute exposure limits.

Figure 2 shows a closed-loop correction of the aberrations in a normal subject by use of the AO UHR OCT system with light centered at 800 nm with 130-nm optical bandwidth (FWHM). The system was first set to compensate for refractive error of the subject. The wave front for the uncorrected (Fig. 2A) and corrected (Fig. 2D) situation and the associated point-spread functions (PSFs) for the uncorrected (Figs. 2B and 2C) and corrected (Figs. 2E and 2F) cases are indicated; aberrations were corrected up to the fifth order. Figure 2G depicts the evolution of the rms error as well as exemplary aberrations (Z_2^0, defocus; Z_2^2, astigmatism; Z_3^{-3}, trefoil; Z_4^{-4}, fourth-order coma aberration) as a function of time for the same subject.[12] These results show effective measurement and correction of lower- and higher-order aberrations despite the use of ultrabroad-bandwidth light, with a residual uncorrected wave front of $\sim$0.1 μm for a 3.68-mm pupil diameter (see Figs. 2A and 2D). Strehl ratio improvements of a factor of more than 10 (Figs. 2B and 2E) were achieved, resulting in a significantly improved PSF profile (Figs. 2C and 2F).

Figure 3 illustrates the effect of aberration correction in UHR OCT, depicting cross-sectional AO UHR OCT tomograms of a normal human eye in the foveal region across a transverse line of 2.8 mm (600 A-scans, lateral spacing of $\sim$5 μm) for the uncorrected (Fig. 3A) as well as corrected (Fig. 3B) case. Small features within the ganglion cell as well as the inner plexiform layer that might correspond to vessels with 12–22-μm diameter are clearly visualized in the twofold enlarged views (Figs. 3C and 3D). A significant improvement in the signal-to-noise ratio (SNR) of up to 9 dB is clearly visible, yielding a slightly better dynamic range (44 dB in the tomogram) than that achieved with standard UHR OCT (42 dB). The clear visualization of all major intraretinal layers indicates that the axial imaging resolution of 3 μm could be preserved.

In Fig. 4 an aberration-corrected vertical AO UHR OCT tomogram in the parafoveal region across a line of 1.125 mm (600 A-scans, transverse sampling rate of $\sim$2 μm) is depicted. The proportions in Fig. 4A are the same as in Fig. 3A; Fig. 4B shows a twofold enlargement. Intraretinal features probably corresponding to vessels with 7–23- as well as 15-μm diameter are clearly visualized in the ganglion cell and inner plexiform layer (see fourfold enlargement in Fig. 4C) as well as in the choroid (see Fig. 4D and arrows in Fig. 4B). These results clearly indicate an achieved transverse resolution of 5–10 μm. This is an improvement of two to three times compared with the UHR OCT systems used so far that employed a 1-mm beam diameter without AO.[3] The uncorrected tomograms should not be compared with tomograms obtained with standard UHR OCT systems, i.e., systems without AO, because the diameter of the beam entering the eye is approximately four times larger in the present study, and therefore the aberrations of the eye decrease UHR OCT image quality. Assuming a Gaussian beam profile, 5–10-μm transverse resolution at an 800-nm central wavelength should theoretically result in an $\sim$50–200-μm depth of field, defined as two times the Rayleigh range. In practice, the actual depth of field useful in OCT tomograms is larger than this theoretical value.[13]

In conclusion, we have demonstrated, for the first time to our knowledge, that AO can be interfaced to UHR OCT, based on broad-bandwidth (130-nm FWHM) state-of-the-art laser technology, by maintaining the performance of both techniques compared with using them as stand alones. Therefore *in vivo*

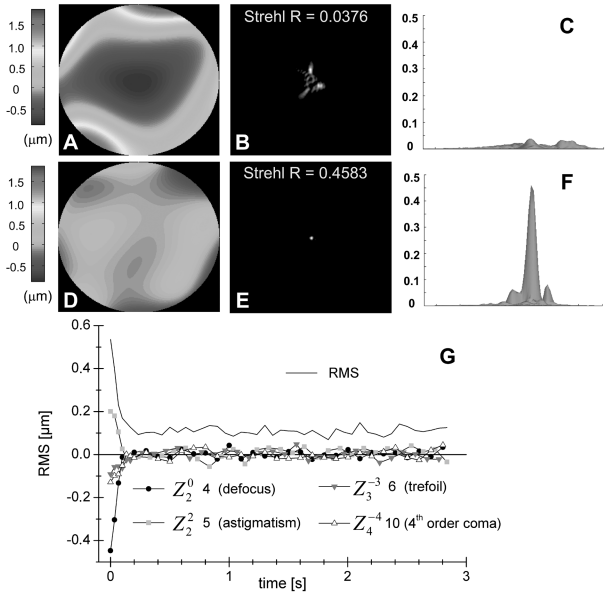

Fig. 2. Wave front for the A, uncorrected and D, corrected case and the associated PSFs for the B, C, uncorrected and E, F, corrected cases are indicated. G, Evolution of the rms error (top, black) of the corrected wave front and representative Zernike coefficients as a function of time for the same subject. A residual uncorrected wave front of $\sim$0.1 μm for a 3.68-mm pupil diameter as well as an improvement of more than ten times of the Strehl ratio is achieved, although using broad-bandwidth (130-nm) light.

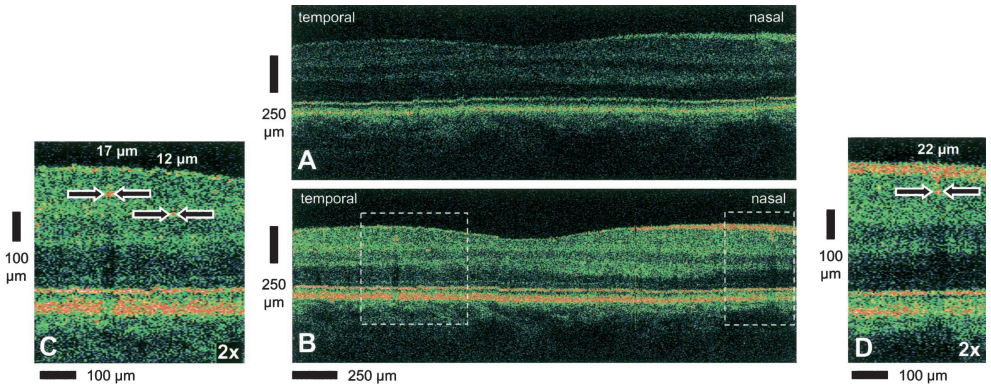

Fig. 3. *In vivo* AO UHR OCT tomograms of a normal human eye in the foveal region for the A, uncorrected as well as B, corrected case (600 A-scans over a line of 2.8 mm, transverse sampling rate of ~5 μm). B, SNR improvement of up to 9 dB as well as 5–10-μm transverse in addition to 3-μm axial resolution could be achieved by wave-front corrections introduced by a 3.68-mm diameter beam. C, D, Small features within the ganglion cell layer, as well as inner plexiform layer, that might correspond to vessels with 12–22-μm diameter are clearly visualized in twofold enlargements.

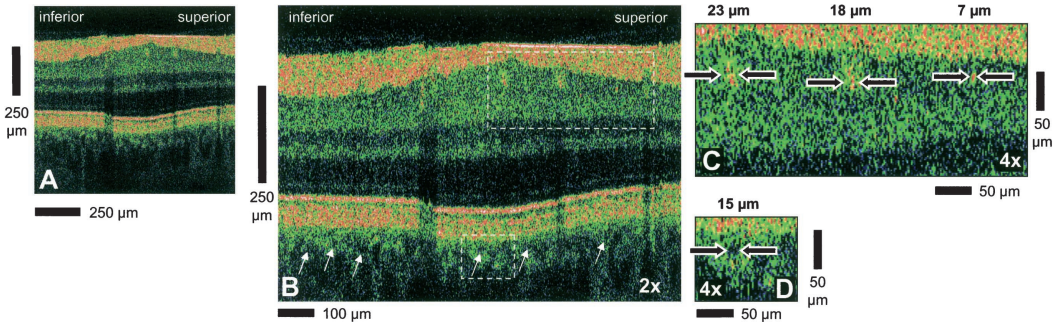

Fig. 4. Aberration-corrected vertical AO UHR tomogram of a normal human eye in the parafoveal region across a line of 1.125 mm (600 A-scans, transverse sampling rate of ~2 μm). The same proportions are used as in Fig. 3A; B is a twofold enlargement of A. Intraretinal features probably corresponding to vessels with 7–23-μm as well as 15-μm diameter are clearly visualized C, in the ganglion cell and inner plexiform layer (fourfold enlargement) as well as D, B (arrows), in the choroid, indicating a transverse resolution of the order of 5–10 μm.

AO UHR OCT imaging of the human retina could be demonstrated with 3-μm axial and 5–10-μm transverse resolution. In addition to improved visualization capabilities, significant UHR OCT tomogram SNR improvements could be obtained. Further improvements of transversal resolution are limited by the approach of the present study to employ a relatively low-cost 37-element micromachined membrane deformable mirror. On the basis of the presented results of this study, however, we expect the development of three-dimensional visualization of retinal features, such as photoreceptors, ganglion cells, or capillaries, by interfacing ultrahigh resolution OCT to AO with corrector devices with improved performance.

We gratefully acknowledge the contributions of L. Schachinger, Medical University of Vienna. This research was supported in part by FWF Y159-PAT, the Christian Doppler Society, FEMTOLASERS Produktions GmbH, Carl Zeiss Meditec AG, MCyT_BFM-001-0391 (Spain), and Acción Integrada España-Austria HU2002-0011. W. Drexler's e-mail address is Wolfgang.Drexler@meduniwien.ac.at.

References

1. D. Huang, E. A. Swanson, C. P. Lin, J. S. Schuman, W. G. Stinson, W. Chang, M. R. Hee, T. Flotte, K. Gregory, C. A. Puliafito, and J. G. Fujimoto, Science **254,** 1178 (1991).
2. W. Drexler, J. Biomed. Opt. **9,** 47 (2004).
3. W. Drexler, U. Morgner, R. K. Ghanta, F. X. Kärtner, J. S. Schuman, and J. G. Fujimoto, Nat. Med. **7,** 502 (2001).
4. P. Artal, A. Guirao, A. Berrio, and D. Williams, J. Vis. **1,** 1 (2001).
5. P. Artal and R. Navarro, Opt. Lett. **14,** 1098 (1989).
6. J. Liang, D. R. Williams, and D. T. Miller, J. Opt. Soc. Am. A **14,** 2884 (1997).
7. F. Vargas-Martín, P. M. Prieto, and P. Artal, J. Opt. Soc. Am. A **15,** 2552 (1998).
8. E. J. Fernandez, I. Iglesias, and P. Artal, Opt. Lett. **26,** 746 (2001).
9. A. Roorda, F. Romero-Borja, W. J. Donnelly III, H. Queener, T. J. Hebert, and M. C. W. Campbell, Opt. Express **10,** 405 (2002), http://www.opticsexpress.org.
10. D. T. Miller, J. Qu, R. S. Jonnal, and K. Thorn, Proc. SPIE **4956,** 65 (2003).
11. E. J. Fernández and P. Artal, Opt. Express **11,** 1056 (2003), http://www.opticsexpress.org.
12. L. N. Thibos, R. A. Applegate, J. T. Schwiegerling, and R. Webb, in *Vision Science and Its Applications*, V. Lakshminarayanan, ed., Vol. 35 of OSA Trends in Optics and Photonics Series (Optical Society of America, Washington, D.C., 2000), pp. 232–244.
13. W. Drexler, U. Morgner, F. X. Kärtner, C. Pitris, S. A. Boppart, X. D. Li, E. P. Ippen, and J. G. Fujimoto, Opt. Lett. **24,** 1221 (1999).